PCCP

Cite this: *Phys. Chem. Chem. Phys.*, 2011, **13**, 15803–15809

www.rsc.org/pccp

PAPER

Interaction of hydrogen with surfaces of silicates: single crystal *vs.* amorphous†

Jiao He, Paul Frank and Gianfranco Vidali*

Received 18th May 2011, Accepted 7th July 2011
DOI: 10.1039/c1cp21601e

We have studied how the formation of molecular hydrogen on silicates at low temperature is influenced by surface morphology. At low temperature (<30 K), the formation of molecular hydrogen occurs chiefly through weak physical adsorption processes. Morphology then plays a role in facilitating or hindering the formation of molecular hydrogen. We studied the formation of molecular hydrogen on a single crystal forsterite and on thin films of amorphous silicate of general composition $(Fe_xMg_{(x-1)})_2SiO_4$, $0 < x < 1$. The samples were studied *ex situ* by Atom Force Microscopy (AFM), and *in situ* using Thermal Programmed Desorption (TPD). The data were analysed using a rate equation model. The main outcome of the experiments is that TPD features of HD desorbing from an amorphous silicate after its formation are much wider than the ones from a single crystal; correspondingly typical energy barriers for diffusion and desorption of H, H_2 are larger as well. The results of our model can be used in chemical evolution codes of space environments, where both amorphous and crystalline silicates have been detected.

1. Introduction

The catalytic role of surfaces at low temperature is an important topic in surface physics as well as in the understanding of the chemical evolution of the interstellar medium.[1–3] In the former case, there is much to be learned, since different physical/chemical processes can be distinguished and quantified. In the latter case, it is now recognized that the surface of an interstellar dust grain is an important locus in the formation of key molecular species found in interstellar space, from hydrogen, the most abundant molecule in the Universe, to formaldehyde and methanol, precursors to molecules of biogenic interest.[4]

In astrochemistry, the study of the formation of molecular hydrogen is an important and active topic of research, since molecular hydrogen intervenes, in the neutral state or charged, in most of the reaction networks to produce more complex molecules,[5,6] and it is also indispensable in the cooling of a gravitationally collapsing cloud by removing energetic photons and re-radiating in the infrared, where the cloud is transparent. Because of the cooling action of molecular hydrogen, the cloud can further proceed to collapse into a protostar.[7]

Interstellar dust is made of carbonaceous material and silicates.[8] One of the most important classes of silicates is of the type $(Fe_xMg_{(x-1)})_2SiO_4$, $0 < x < 1$. Mg rich silicates are called forsterite and the Fe rich are fayalite. A common name for the mineral found on Earth is olivine.

Silicates are detected in emission and absorption in the mid-IR through Si–O stretching and the O–Si–O bending mode at 9.7 and 18 μm. Infrared spectroscopic work using satellites, such as ISO (Infrared Space Observatory), coupled with measurements in the laboratory, found that in the interstellar medium (ISM) silicates are amorphous (or glassy), while in the circumstellar environments of pre- and post-main-sequence stars a fraction that can be as high as 20% is in the crystalline form.[9] In the solar system, as well as in protoplanetary disks, crystalline silicates are typically found. In this case, it is speculated that the silicates become crystalline through high temperature annealing in protoplanetary/presolar environments.

A large amount of work has been done to study in the laboratory the properties of man-made silicates and to then compare them with infrared signatures from space.[10–12] In the research described in this paper, the catalytic properties of amorphous silicates are compared with the ones of a single crystal in order to gauge the role of surface order in the formation of molecules. These results can then be used to predict the efficiency of molecule formation on silicates in different interstellar or planetary environments. With a similar goal, studies of surface morphology of materials of astrophysical interest were carried out on amorphous water ice[13,14] and other ices.[15] More generally, studies of hydrogen adsorption on and desorption from other porous materials were done, for example, by Panella *et al.*[16] and Volkringer *et al.*[17]

In the past, we extensively studied the formation of molecular hydrogen on amorphous silicate surfaces.[18–21] We found that the interaction of hydrogen atoms and molecules with surfaces of silicates at low temperature (<30 K) is dominated by weak adsorption forces. TPD experiments after

Syracuse University, Physics Department, Syracuse, NY 13244-1130, USA. E-mail: gvidali@syr.edu
† This article was submitted as part of a collection following the Low Temperature Spectroscopy/Kuiper Belt Objects symposium at Pacifichem2010.

irradiation of the surface with H and D neutral atoms resulted in HD features that were broad. We used a variety of methods, already described in the literature and summarized below, to obtain activation energies of diffusion of single atoms and desorption energies of atoms and molecules. The mechanisms of reaction were studied too. It was found that the Eley–Rideal reaction, in which an atom impinges directly on another atom on the surface resulting in the formation of a molecule without prior accommodation with the surface, is not the main mechanism of HD formation, at least in the range of parameters explored, well below monolayer coverage of H or D and surface temperature between 5 and 30 K. Rather from an analysis of our experimental results we conclude that the Langmuir–Hinshelwood reaction can explain most of the results.[22] However, in a recent experiment of D + D → D_2 formation on a optically flat silicate film, Lemaire *et al.*[23] found that 3.5% of D_2 molecules are formed in the $\nu = 4, J = 2$ excited state and they estimated that up to 30% of the molecules formed on the surface are in an excited state. The remaining fraction comes off during the TPD. What fraction of molecules is in excited states likely depends on the condition of the surface. Too few experiments that measure the ro-vibrational or translational states of molecules have been done to draw conclusions; it appears that on rough, porous surfaces, such as amorphous water ice, desorption is near thermal,[24,25] but on graphite[26] and on a smooth silicate film[23] molecules come out in excited states. A model about formation-driven excitation of H_2 based on recent experiments is given by Islam *et al.*[26]

In our experiments on rough amorphous ice and silicate surfaces, we found that thermal energy was needed to initiate the reaction, meaning that tunnelling *alone* was not sufficient.[22,27] This is understandable, considering that tunnelling is very sensitive to the height and width of the energy barrier separating adjacent sites. Because of the amorphous nature of the films, it is conceivable that there are deep adsorption sites for H and D that act as traps, similarly to the problem of electron conduction in amorphous silicon. Indeed, while a calculation by Hollenbach and Salpeter[28] showed that the motion of an H atom on a polycrystalline water ice is fast due to tunnelling, Smoluchowski[29] found that H motion in amorphous ice is very slow. His calculation gave a value of the efficiency of H_2 formation that was much too small to justify the abundance of H_2 in the interstellar medium where it is photodissociated at a known rate and thus has to be made at the same rate for the maintaining of steady state conditions.[30] This was the motivation to study in the laboratory the formation of H_2 on interstellar grain analogues under space environments conditions. Now we report the results of a study to evaluate how the structure of the surface of a silicate, crystalline *vs.* amorphous, affects the formation of H_2. Information gained in this study helps modellers of the chemical evolution of interstellar medium environments;[31] we also get a glimpse on processes of hydrogen–surface interaction at low (~10 K) surface temperature.

2. Experimental

The apparatus used in these experiments consists of a main chamber that houses the sample and a quadrupole mass spectrometer, and two beamlines, each of which can be pumped independently.[32] The main chamber is pumped by a cryopump, turbo pumps and an ion pump, yielding the pressure of 1×10^{-10} Torr after the bake-out. The sample is mounted on a cold finger attached to a doubly differentially-pumped rotatable platform. The temperature of the sample is measured by a calibrated LakeShore silicon diode thermometer located right behind the sample and can be heated by a cartridge heater in the sample holder or by regulating the flow of liquid helium. Typically the heater is used to maintain a set temperature of the sample during the irradiation process while during the TPD experiments the temperature of the sample is changed by cutting off the flow of liquid helium. For the experiments presented in this paper, two different types of samples were used, a single crystal of olivine (dimensions $10 \times 10 \times 3$ mm^3) and amorphous thin films of silicates deposited on $\frac{1}{2}''$ diameter copper disks. The thin film samples were prepared by Dr John Brucato of the Arcetri Astronomical Observatory in Italy. Thin amorphous silicate films of different composition ($(Fe_xMg_{1-x})_2SiO_4$ ($0 < x < 1$)) were made by laser ablation (wavelength 266 nm) of a mixed MgO, FeO and SiO_2 target in an oxygen atmosphere (10 mbar) and were deposited on 0.5 inch diameter OFHC copper disks. The optical and stoichiometric characterization of the samples produced with this technique is given elsewhere.[12] Results and analysis of molecular hydrogen formation have been published before.[19,20] Here we use samples with composition Fe_2SiO_4 and $FeMgSiO_4$ (the silicate films yield similar TPD features—see below—although the efficiency of H_2 formation might vary depending on the surface disorder).[16] The silicate single crystal, an olivine ($FeMgSiO_4$) with the (100) surface exposed, was kindly provided by Dr Sergei Kucheyev of the Livermore National Laboratory. The samples were mounted on a sample holder whose temperature could be changed in the range of 5 K to 800 K. AFM images of the single crystal and the amorphous olivine are shown in Fig. 1. The single crystal is flat with a peak-to-peak surface roughness of less than 5 nm over a 10 micron range. The surface irregularities of the amorphous silicate are higher by some orders of magnitude up to a micron.

The single crystal silicate was anchored to a sample holder that was connected to the cold finger *via* an Advanced

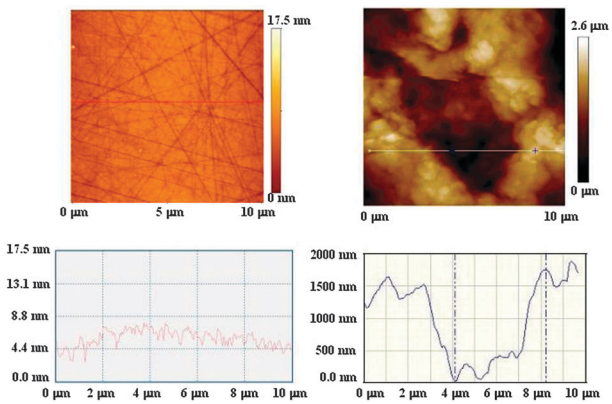

Fig. 1 AFM images and line scans of single crystal silicate (left) and amorphous silicate (right).

Research Systems 800 K stage. This stage was used to thermally decouple the cold stage from the sample during extended heating of the latter. Due to the single crystal silicate poor heat conductivity the temperature measured at the backside of the sample might be different from the temperature at the front side where the reactions actually take place. Therefore the temperature measured by the silicon diode (the nominal sample temperature) has to be checked and corrected when appropriate. The correction procedure is described in the Appendix.

Because of the fragility of the thin films, no *ex situ* chemical cleaning was used. Instead, the samples were heated repeatedly during the bake of the UHV chamber, and prior to each experiment, to 380 K. According to a calculation of the stability of single crystal silicates (forsterite, Mg_2SiO_4) to water adsorption, a chemisorbed layer of water is expected to be present at the low index faces of fosterite.[33,34] The calculated binding energies of water on such surfaces are in the range of 1 eV for most low-index faces. In a TPD experiment, we would expect to find a water desorption peak at 350–400 K, according to the calculations. No water was found to desorb from the amorphous silicate before 380 K as measured by our quadrupole mass spectrometer. Heating beyond 450 K, while still yielding no water, resulted in the destruction of the sample during cooling, probably because of mechanical stresses between the film and the substrate. The single crystal was taken to over 600 K, again without emergence of water. In these experiments, short dosing times were used. From preceding work we know that in doing so, the typical coverage is a small fraction (1–10%) of a monolayer.[15] The triple pass Hiden quadrupole mass spectrometer (QMS) is mounted on a double differentially rotatable platform and can therefore be used not only to check the reaction products, but also to measure purity, flux and dissociation efficiency of the incoming beams. In a typical experiment the sample is kept at the desired temperature until the temperature has stabilized. The QMS sensitivity diminishes for fast particles. Thus, our detector underestimates the contribution from excited molecules with high translational energy. Presently, it is not known what the translational energy of excited molecules formed on surfaces is, except for HD formed on amorphous water ice, where the translational energy is nearly thermal.[24,25] Thereupon the sample is exposed to the beams for a short time (the "irradiation phase", lasting typically from 30 s to 4 min) and the QMS, placed in front of the sample and in between the beam-lines, detects the composition of gases evolving from the sample. After closing the beam-line valves, the flow of liquid helium is cut which leads to a rapid and reproducible increase of the surface temperature (desorption phase). Typically the temperature is left to rise to 50–60 K before restarting the liquid helium flow. Periodically the sample is heated up without being exposed to the beams (dry runs) in order to check back adsorption of gases that have not been pumped away quickly enough.

3. Results and discussion

First, experiments were done to quantify the differences between the single crystal and the amorphous film in terms of the landscape of adsorption/desorption sites. In a previous work, we studied the adsorption and desorption of D_2 molecules to obtain the distribution of adsorption/desorption energies.[21] Here we do the same for the single crystal. Then, the results of the formation of HD on the single crystal were studied and compared with the results from an amorphous silicate.

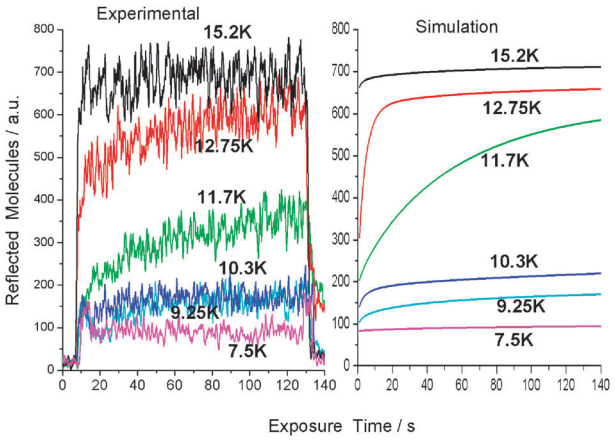

Fig. 2 The QMS mass-4 signal (reflected deuterium molecules) during irradiation at different sample temperatures. Experiment data at left, simulated traces at right (see Appendix).

3.1 Adsorption/desorption of D_2

There are two distinct phases of the experiments: the phase of irradiation of the sample with atoms/molecules and the desorption phase.

In the irradiation phase, hydrogen and deuterium atoms or molecules are introduced for a given amount of time, usually 30 s to 4 min, yielding a coverage on the surface of a small fraction of a layer (assuming that every atom sticks). Fig. 2 (left panel) shows the quadrupole mass spectrometer signal proportional to D_2 molecules that are reflected from the surface. As the experiment is done at higher surface temperature more molecules are detected because fewer stick. Therefore, an analysis of this measurement gives the sticking coefficient. Immediately after each irradiation, the surface temperature is rapidly raised so molecules desorb or atoms diffuse, react and the resulting molecules desorb. Fig. 3 shows typical TPD traces after irradiation of D_2 for 2 minutes at $\sim$7 K. As mentioned in the previous section, the temperature ramp is most reliably obtained by shutting the flow of liquid helium, giving a very reproducible temperature increase. Similar results are obtained using the heater while keeping the liquid helium flowing. The slope of temperature *vs.* time dT/dt is calculated and used to convert the measured QMS signal dN/dt to dN/dT.

3.2 Analysis of data

To analyse the data we use a rate equation model.[18] The number of deuterium molecules on the single crystal surface during the irradiation stage can be expressed by the following formula

$$\frac{dN}{dt} = f - \nu N \exp\left(-\frac{E_d}{kT}\right) \quad (1)$$

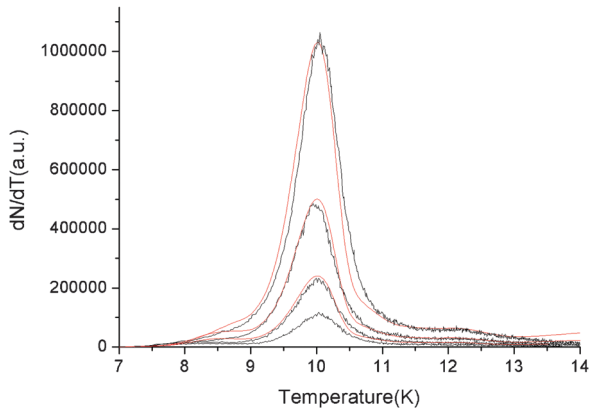

Fig. 3 Desorption of D_2 from the single crystal silicate. The exposure time is (bottom to top) 2 min, 4 min, 8 min, 16 min, respectively. The black curves are the experimental curves and the red curves are the fits (see text).

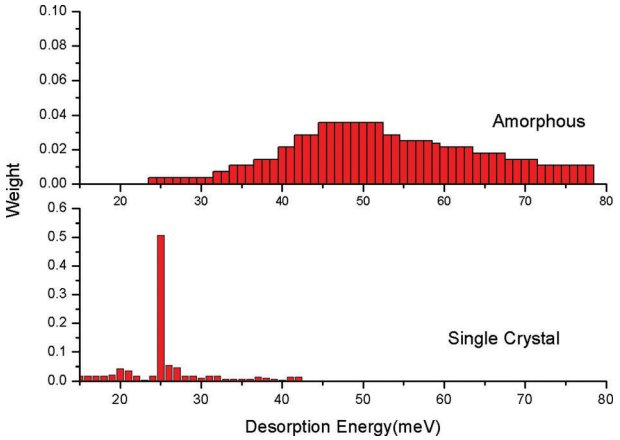

Fig. 4 Distribution of desorption energy of D_2 from the amorphous silicate (top) and the single crystalline silicate (bottom).

where f is the incoming flux, the second term represents the desorption of molecules from the surface, ν is the attempt rate which is taken to be 10^{12} s^{-1} [14], E_d is the desorption energy barrier for deuterium molecules, T is the temperature of the surface. Solving this equation we can get

$$N(t) = \frac{f}{\left(\nu \exp\left(-\frac{E_d}{kT}\right)\right)\left(1 - \exp\left(-t\nu \exp\left(-\frac{E_d}{kT}\right)\right)\right)}$$

The number of molecules desorbed from the surface, which is proportional to the signal from the QMS, is

$$\nu N \exp\left(-\frac{E_d}{kT}\right) = f\left(1 - \exp\left(-t\nu \exp\left(-\frac{E_d}{kT}\right)\right)\right) \quad (2)$$

If the exposure time is long enough, $t \rightarrow +\infty$, the desorption term will be f, which means that all the sites on the surface are occupied, and the sticking efficiency becomes 0 (above this temperature there is little or no D_2 signal in the TPD, indicating that there are no molecules left on the surface).

We then simulate the TPD process. In eqn (1) we make explicit the dependence of the flux $f(t)$ and the temperature $T(t)$ with time.

$$f(t) = \begin{cases} f & t \le t_0 \\ 0 & t > t_0 \end{cases}$$

$$T(t) = \begin{cases} T0 & t \le t_0 \\ T0 + \frac{a(t-t_0)+b}{c+(t-t_0)} + d(t-t_0)^{\frac{1}{3}} & t > t_0 \end{cases}$$

where t_0 is the time when the beam valve is closed and the helium flow is cut off, $T0$ is the irradiation temperature. For each experiment we need to find the best fit parameters for a, b, c, d and $T0$ in the above function. Since there are adsorption sites with different energy barriers on the surface, we need to modify the rate equation so that it can be used for the case with multiple values of the energy.

$$\frac{dN_i(t)}{dt} = p_i f(t) - \nu N_i(t) \exp\left(-\frac{E_{di}}{kT(t)}\right)$$

$$N(t) = \sum N_i(t)$$

$$\sum p_i(t) = 1$$

The measured QMS signal is proportional to $\sum \nu N_i(t) \exp\left(-\frac{E_{di}}{kT(t)}\right)$. We solve the differential equations and the simulation result is fitted to the experimental data by carefully adjusting the energies E_{di} and their weights p_i. This distribution of energy is put into eqn (2) and we generate a reflection trace for the irradiation phase

$$\sum p_i f\left(1 - \exp\left(-t\nu \exp\left(-\frac{E_{di}}{kT}\right)\right)\right)$$

The red line in Fig. 3 shows a fit of a TPD experiment by solving the rate equations; one can see that most of the deuterium molecules desorbed at temperature from 9 K to 11 K. The bottom of Fig. 4 shows the distribution of desorption energies of deuterium molecules from the single crystal silicate. The distribution is centred around 25 meV. This energy peak compares well with an independent measurement of HD desorbing from polycrystalline olivine (peak at 10–12 K)[22] and with D_2 desorbing from a flat silicate film (maximum yield $< \sim 12$ K).[23]

Similar TPD experiments were done with amorphous silicate samples. The samples were exposed to a flux of D_2 molecules for 4 minutes, and the exposure temperature is 12 K. A typical dN/dT as a function of temperature is shown in Fig. 5. Comparing it with Fig. 3, we can see that the TPD curve covers a much broader temperature range than the one from the single crystalline silicate surface. From Fig. 4 one can see that the activation energies for desorption from the amorphous silicate are higher than from the single crystal; furthermore, the distribution is skewed, with a large number of deeper adsorbing sites on the amorphous silicate surface.

That there is a wide distribution of desorption energies of D_2 from amorphous materials at low temperature was also found by Amiaud *et al.*[35] and by Perets *et al.*[36] in the analysis of D_2 desorption from compact amorphous water ice and porous amorphous water ice.

3.3 Molecular hydrogen formation

Next we study the formation of molecule hydrogen on a silicate surface. H atoms and D atoms are sent to the sample

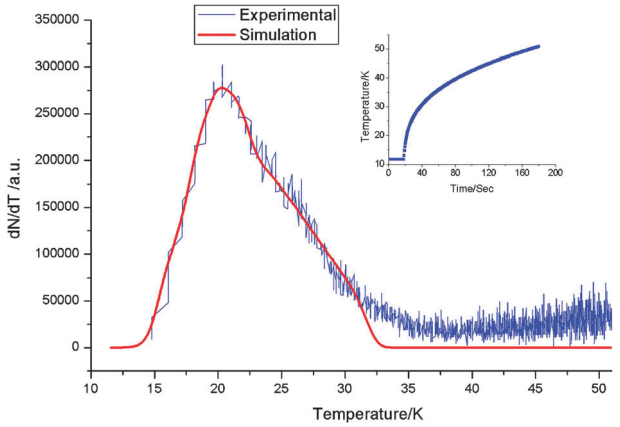

Fig. 5 Desorption of D_2 from an amorphous silicate; the temperature *vs.* time curve is in the inset. The experimental trace is in blue, while the red curve is the fit. The rise of the trace at high temperature is due to noise in the conversion dN/dt to dN/dT.

in the main chamber through two beam lines. There are three chemical reactions involved:

$$H + H \rightarrow H_2$$

$$D + D \rightarrow D_2$$

$$H + D \rightarrow HD$$

We write the rate equations for H and D atoms and for H_2, D_2 and HD molecules. Here are the ones for H and H_2:

$$\begin{aligned}\frac{dN_H(t)}{dt} &= f_H(t) - \nu N_H(t)\exp\left(-\frac{E_H}{kT(t)}\right) \\ &\quad - 2\nu\frac{\pi r^2}{A}N_H^2(t)\exp\left(-\frac{e_H}{kT(t)}\right) \\ &\quad - \nu\frac{\pi r^2}{A}N_H(t)N_D(t)\exp\left(-\frac{e_{HD}}{kT(t)}\right)\end{aligned} \quad (3)$$

$$\begin{aligned}\frac{dN_{H2}(t)}{dt} &= \nu\frac{\pi r^2}{A}N_H^2(t)\exp\left(-\frac{e_H}{kT(t)}\right) \\ &\quad - \nu N_{H_2}(t)\exp\left(-\frac{E_{H_2}}{kT(t)}\right)\end{aligned} \quad (4)$$

In eqn (3) the first term on the right side is the flux, the second is the desorption term for atoms, E_H is the desorption energy. The third is the diffusion term due to the reaction H + H → H_2, the factor 2 arising from the fact that two atoms form one molecule. e_H is the diffusion energy of H atoms. We assume that one atom can only react with another atom within a distance of r, A is the total area of the sample, then for each atom there are $\frac{\pi r^2}{A}N_H$ located within this range, and the diffusion is proportional to this term.[37] In our case, A is taken to be 1 cm^2 and r is 0.2 nm, or about 3 times of the H–H bond length. The exact value of r will not affect the final result of diffusion energy too much since the diffusion energy is in the exponential term. The fourth term in eqn (3) is due to the reaction H + D → HD. In eqn (4) the first term on the right side is the gain from the H + H reaction. The second term is the desorption term for hydrogen molecules. E_{H_2} is the H_2 desorption energy. For further details, see ref. 18. In the experiment, mass 3 (HD) and mass 4 (D_2) are measured and compared with simulation results, since mass 2 (H_2) has contributions from the background.

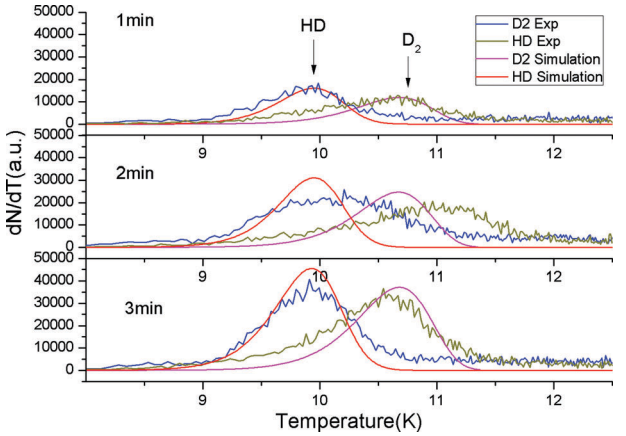

Fig. 6 TPD of H + D from the single crystal. The irradiation times are 1 min, 2 min, 3 min and the sample temperature is 7 K.

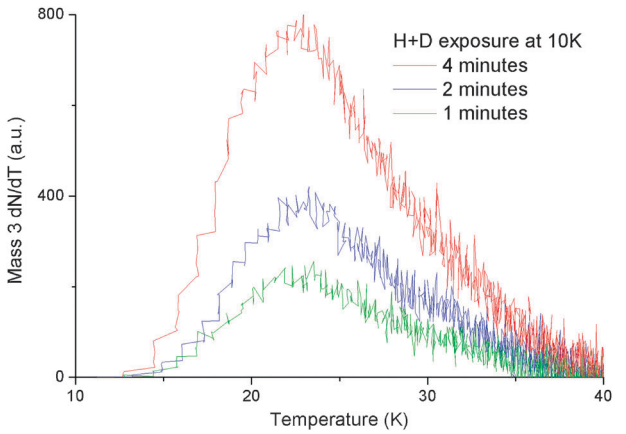

Fig. 7 TPD of H + D from the amorphous silicate. Adsorption temperature 10 K, exposure times of 1 min (green), 2 min (blue) and 4 min (red).

In the simulation, in order to keep the number of parameters low, we don't differentiate between H and D except for the desorption of molecules. By comparing the simulation results and the experimental TPD curve, see Fig. 6, we found that the diffusion energy barrier is 8.5 meV for atoms (if we assume thermal activation[37]), the desorption energy for HD is 24.5 meV, and the desorption energy for D_2 is 27 mev.

Similar experiments were carried out on an amorphous silicate sample (Fig. 7). For the single crystal, there is a main peak at about 10 K while for the amorphous olivine there is a wide TPD yield between 10 K and 35 K. An analysis using a similar model but fitting the TPDs with three main energies gave the desorption energy of HD of 35, 53, and 75 meV and the energy for diffusion of H of 35 meV.[19]

4. Conclusions

The difference in the kinetics of H + D formation in amorphous *vs.* single crystal silicates is rather dramatic. While HD

molecules that are formed on the surface of an amorphous silicate have desorption energies of around 60 meV, this energy is much less on polycrystalline silicate (a telluric sample of olivine) 27 meV, and even smaller here, 25 meV. The activation energy for diffusion on a crystalline surface is also lower, 8.5 meV (if we assume thermal activation) compared to 35 meV in the case of an amorphous silicate. Obviously, as pointed out before when we made a comparison of results from an amorphous silicate with the ones from a polycrystalline olivine[19] this makes a difference in the formation of molecular hydrogen on dust grains in actual space environments. The calculated efficiency of molecular hydrogen formation on grains in steady state conditions is high over a dust temperature range that for amorphous grains is shifted to higher temperature than for polycrystalline.[18] For crystalline silicates, this window is shifted even lower than for polycrystalline silicates, thus making the formation of molecular hydrogen problematic in this case, and, by extension, where crystalline silicates are present.[9,30,31] When there is no chemisorption, it is expected that this trend be verified also for the formation of other molecules, especially the ones formed by hydrogen addition reactions.[32] In the light Lemaire *et al.*'s experiments on a smooth silicate film,[23] it is possible that on the single crystal forsterite there is a fraction of molecules formed in high ro-vibrational states. However, a conservative estimate of the yield of HD molecules detected in our experiment during the irradiation is 25% of the total yield. Nonetheless, similarly to the *estimate* in Lamaire's work,[23] the largest fraction of molecular hydrogen formed on the surface is during the TPD phase. It would be interesting to measure both fractions as a function of surface morphology, as this measurement would have implications for understanding the formation of molecular hydrogen in interstellar space.

Appendix

Methods

One of the challenges in making measurements of surface processes at low temperature is to obtain reliable reading of the temperature of the sample. By using a combination of a calibrated silicon diode and of gold/iron-constantan thermocouples placed in different locations around the sample, it was possible to obtain reliable sample temperatures of samples consisting of micron thick films of silicates deposited on copper disks that were firmly fastened to an OFHC copper sample holder.[32] A thin layer of indium improved the thermal contact between the various surfaces of the sample holder. Because of the size and thickness of the single crystal, the measurement of its temperature required to be verified and corrected. This was done using irradiation and desorption data from experiments with deuterium molecules.

Below is a summary of this temperature correction procedure that is done using the experiments with D_2 adsorption/desorption. We found that this method is very robust and it capitalizes on our experience with analyzing TPD traces at these low temperatures.

We run the rate equation simulation and find the desorption energy distribution by fitting the TPD curve. Fig. 3 shows how a typical fitting looks like.

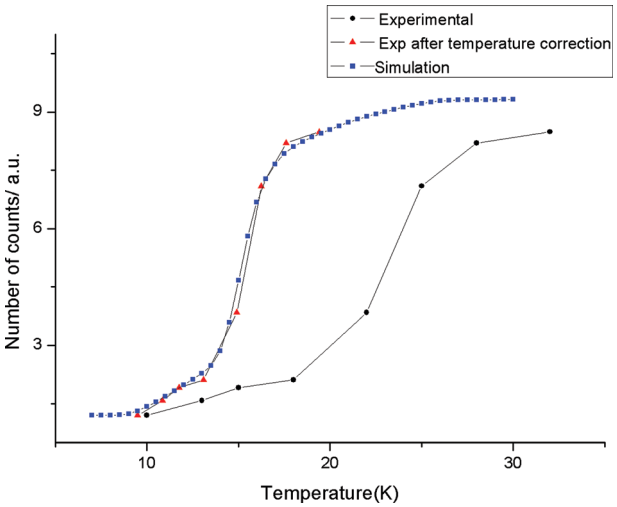

Fig. 8 Integrated number of counts during irradiation *versus* irradiation temperature.

We apply the obtained energy distribution, like in Fig. 4, to simulate the adsorption (irradiation) trace and generate the number of reflected deuterium molecules as a function of time at a given exposure temperature, Fig. 2, right panel. We then integrate it, thus obtaining the total number of reflected molecules during the irradiation stage at that irradiation temperature. We repeat this procedure for all the exposure temperatures.

A procedure as described above is applied to the signal. We then plot the integrated signals obtained at different temperatures *vs.* the irradiation temperature. The same is done for the simulated traces. The two curves (integration of signal *vs.* irradiation temperature and integration of simulated signal *vs.* irradiation temperature) are compared and brought together by finding an appropriate formula of temperature correction. Here a linear formula is adopted which reflects that the temperature gradient is a linear function of temperature. Fig. 8 shows one of the fittings.

We apply the temperature correction formula to modify all the measured temperatures in the TPD experiments including the irradiation phase. We then repeat until convergence is obtained. As it happens, the convergence is rapid.

The corrections yield results that are in agreement with previous results using a polycrystalline olivine[17] (Note that Fig. 6 of ref. 21 has an incorrect temperature scale). The figures presented above have all the corrected temperature values.

Acknowledgements

This work was supported in part by a grant from the NSF Astronomy and Astrophysics Division (0908108). We thank Dr John Brucato (Arcetri Astronomical Observatory) for providing the amorphous samples and Dr Sergei Kucheyev of the Livermore National Laboratory for the crystal silicate.

References

1 D. A. Williams and E. Herbst, *Surf. Sci.*, 2002, **500**, 823–837.
2 H. J. Fraser and E. F. van Dishoeck, *Space Life Sci.*, 2004, **33**, 14–22.
3 A. Lakhlifi and J. P. Killingbeck, *Surf. Sci.*, 2010, **604**, 38–46.

4 E. Herbst and E. F. van Dishoeck, *Annu. Rev. Astron. Astrophys.*, 2009, **47**, 427–480.
5 F. Combes and G. Pineau des Forets, *Molecular Hydrogen in Space*, Cambridge University Press, Cambridge, 2000.
6 E. Herbst, *Chem. Soc. Rev.*, 2001, **30**, 168–176.
7 D. A. Williams and T. W. Hartquist, *Acc. Chem. Res.*, 1999, **32**, 334–341.
8 B. T. Draine, *Annu. Rev. Astron. Astrophys.*, 2003, **41**, 241–289.
9 F. Molster and C. Kemper, *Space Sci. Rev.*, 2005, **119**, 3–28.
10 T. Henning, *Annu. Rev. Astron. Astrophys.*, 2010, **48**, 21–46.
11 L. Colangeli, T. Henning, J. R. Brucato, D. Clement, D. Fabian, O. Guillois, F. Huisken, C. Jager, E. K. Jessberger, A. Jones, G. Ledoux, G. Manico, V. Mennella, F. J. Molster, H. Mutschke, V. Pirronello, C. Reynaud, J. Roser, G. Vidali and L. Waters, *Astron. Astrophys. Rev.*, 2003, **11**, 97–152.
12 J. R. Brucato, V. Mennella, L. Colangeli, A. Rotundi and P. Palumbo, *Planet. Space Sci.*, 2002, **50**, 829–837.
13 P. Ayotte, R. S. Smith, K. P. Stevenson, Z. Dohnalek, G. A. Kimmel and B. D. Kay, *J. Geophys. Res.*, 2001, **106**, 33387–33392.
14 L. Amiaud, F. Dulieu, J. H. Fillion, A. Momeni and J. L. Lemaire, *J. Chem. Phys.*, 2007, **127**, 144709.
15 D. J. Burke and W. A. Brown, *Phys. Chem. Chem. Phys.*, 2010, **12**, 5947–5969.
16 B. Panella, M. Hirscher and B. Ludescher, *Microporous Mesoporous Mater.*, 2007, **103**, 230–234.
17 C. Volkringer, T. Loiseau, M. Haouas, F. Taulelle, D. Popov, M. Burghammer, C. Riekel, C. Zlotea, F. Cuevas, M. Latroche, D. Phanon, C. Knofelv, P. L. Llewellyn and G. Ferey, *Chem. Mater.*, 2009, **21**, 5783–5791.
18 H. B. Perets, A. Lederhendler, O. Biham, G. Vidali, L. Li, S. Swords, E. Congiu, J. Roser, G. Manico, J. R. Brucato and V. Pirronello, *Astrophys. J.*, 2007, **661**, L163–L166.
19 G. Vidali, V. Pirronello, L. Li, J. Roser, G. Manico, E. Congiu, H. Mehl, A. Lederhendler, H. B. Perets, J. R. Brucato and O. Biham, *J. Phys. Chem. A*, 2007, **111**, 12611–12619.
20 G. Vidali, L. Li, J. E. Roser and R. Badman, *Adv. Space Res.*, 2009, **43**, 1291–1298.
21 G. Vidali and L. Li, *J. Phys.: Condens. Matter*, 2010, **22**, 304012.
22 V. Pirronello, O. Biham, C. Liu, L. O. Shen and G. Vidali, *Astrophys. J.*, 1997, **483**, L131–L134.
23 J. L. Lemaire, G. Vidali, S. Baouche, M. Chehrouri, H. Chaabouni and H. Mokrane, *Astrophys. J.*, 2010, **725**, L156–L160.
24 J. E. Roser, S. Swords, G. Vidali, G. Manico and V. Pirronello, *Astrophys. J.*, 2003, **596**, L55–L58.
25 L. Hornekaer, A. Baurichter, V. V. Petrunin, D. Field and A. C. Luntz, *Science*, 2003, **302**, 1943–1946.
26 F. Islam, C. Cecchi-Pestellini, S. Viti and S. Casu, *Astrophys. J.*, 2010, **725**, 1111–1123.
27 N. Watanabe, Y. Kimura, A. Kouchi, T. Chigai, T. Hama and V. Pirronello, *Astrophys. J.*, 2010, **714**, L233–L237.
28 D. Hollenbach and E. E. Salpeter, *Astrophys. J.*, 1971, **163**, 155–164.
29 R. Smoluchowski, *Astrophys. Space Sci.*, 1981, **75**, 353–363.
30 W. Duley and W. A. Williams, *Interstellar Chemistry*, Academic Press, New York, 1984.
31 H. M. Cuppen and E. Herbst, *Mon. Not. R. Astron. Soc.*, 2005, **361**, 565–576.
32 G. Vidali, J. Roser, G. Manico, V. Pirronello, H. B. Perets and O. Biham, *J. Phys. Conf. Ser.*, 2005, **6**, 36–58.
33 T. P. M. Goumans, C. R. A. Catlow, W. A. Brown, J. Kastner and P. Sherwood, *Phys. Chem. Chem. Phys.*, 2009, **11**, 5431–5436.
34 N. H. deLeeuw, *J. Phys. Chem. B*, 2001, **105**, 9747–9754.
35 L. Amiaud, J. H. Fillion, S. Baouche, F. Dulieu, A. Momeni and J. L. Lemaire, *J. Chem. Phys.*, 2006, **124**, 094702.
36 H. B. Perets, O. Biham, G. Manico, V. Pirronello, J. Roser, S. Swords and G. Vidali, *Astrophys. J.*, 2005, **627**, 850–860.
37 J. He, K. Gao, G. Vidali, C. J. Bennett and R. I. Kaiser, *Astrophys. J.*, 2010, **721**, 1656–1662.